Pichlo et al., http://www.jcb.org/cgi/content/full/jcb.201402027/DC1

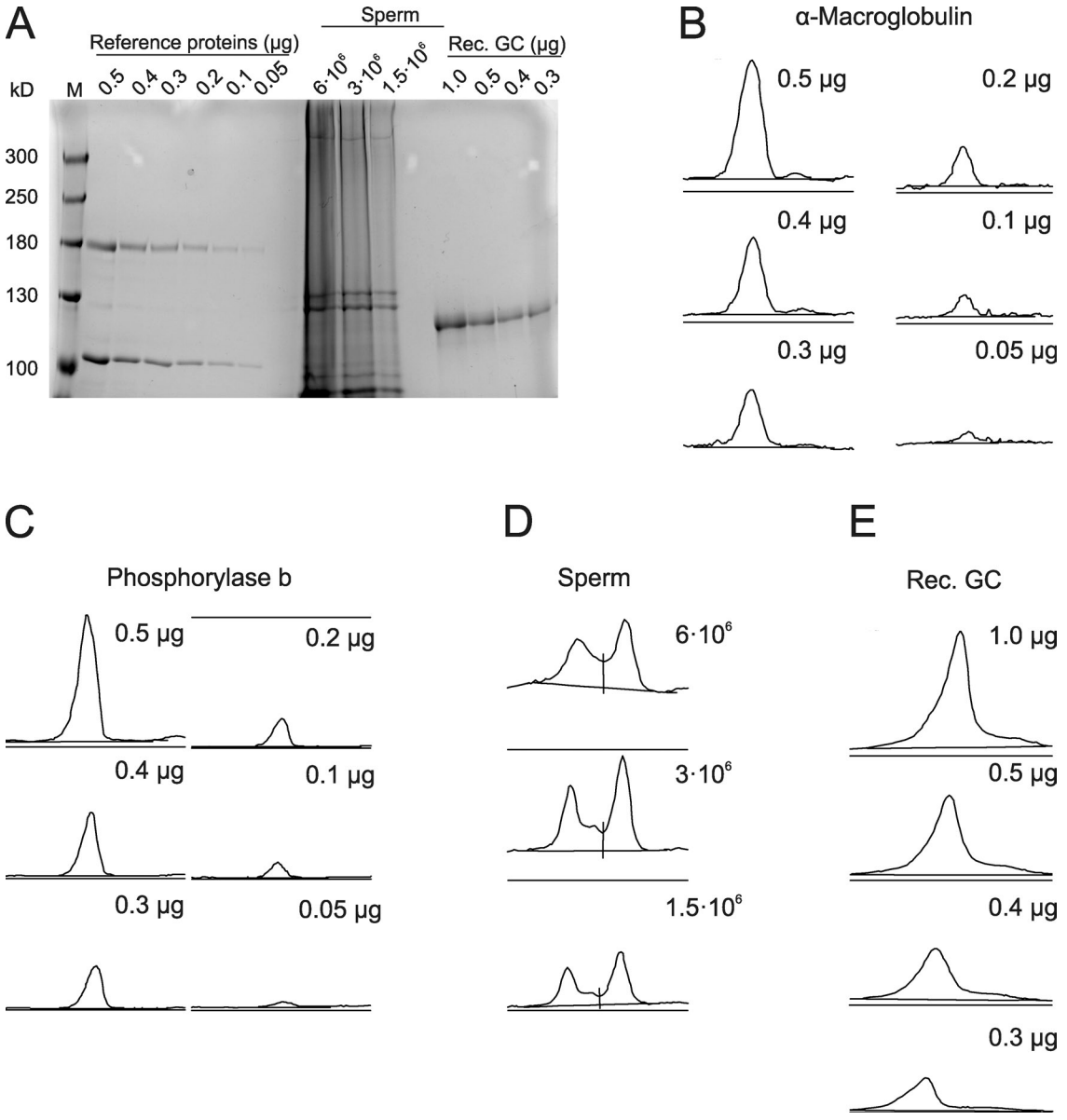

Figure S1. **Densitometric analysis of GC density per sperm cell.** (A) Representative Coomassie-stained SDS polyacrylamide gel used for densitometric determination of GC density. The amount of GC per sperm cell was estimated either by comparison with two standard proteins, phosphorylase b (97 kD) and α-macroglobulin (176 kD), or by comparison with purified recombinant GC (Rec. GC). M, molecular marker. (B–E) Corresponding histograms showing staining intensity of α-macroglobulin (B), phosphorylase b (C), native GC (D), and recombinant GC (E). Histograms were obtained with ImageJ. The sperm sample exhibits two adjacent peaks. The right peak corresponds to the GC, and the left peak corresponds to a sperm-specific isoform of creatine kinase (separated by vertical lines in D).

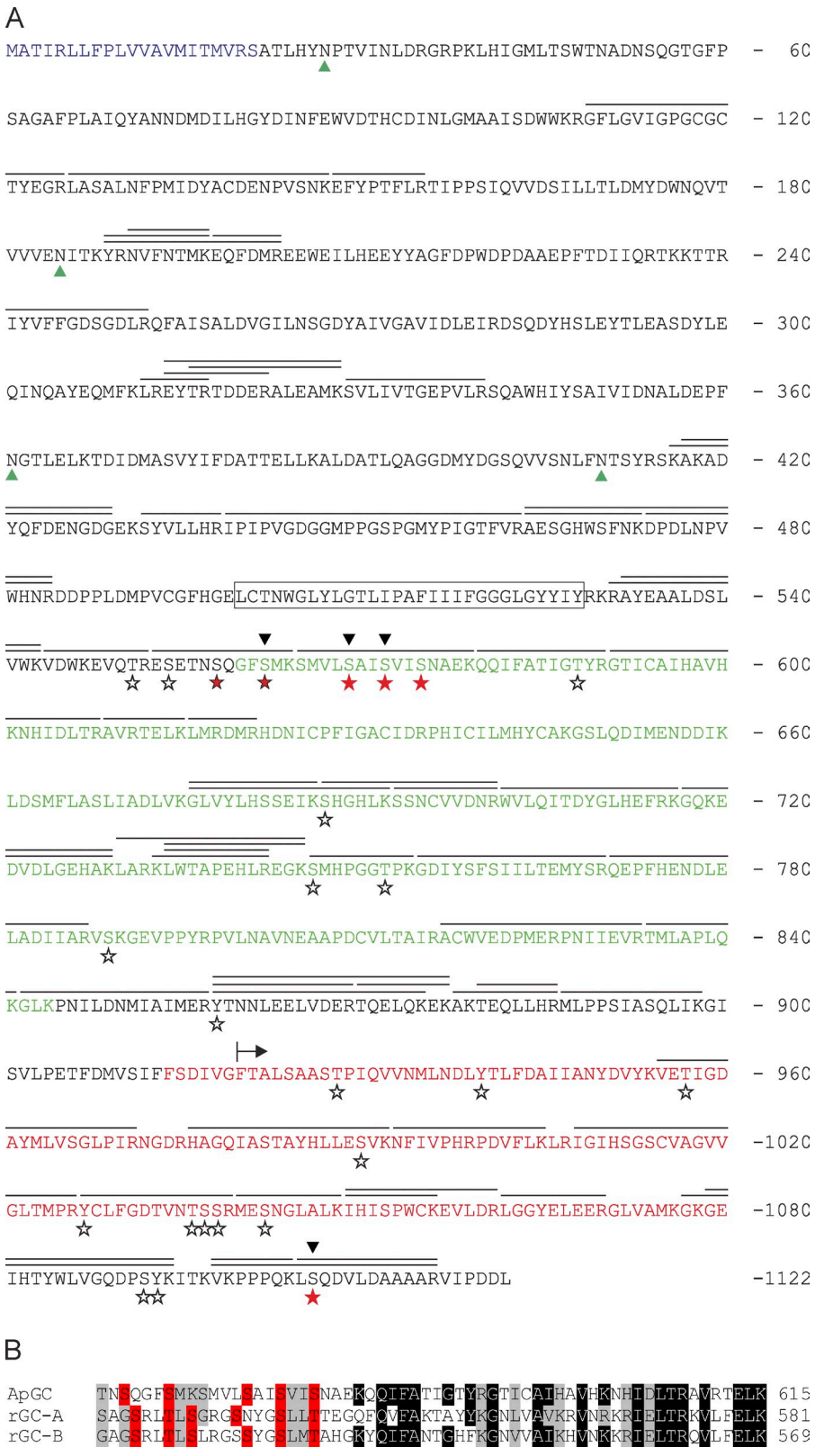

Figure S2. **Primary structure of the GC.** (A) The N-terminal signal sequence (blue), the putative transmembrane segment (boxed), the KHD (green), and the C-terminal catalytic domain (red) are indicated. Potential sites of N-glycosylation (green triangles) and predicted sites for phosphorylation by serine, threonine, and tyrosine kinases (open stars) are indicated. Red stars indicate phosphorylated amino acids identified by MS. Closed arrowheads indicate amino acids that become dephosphorylated after stimulation with resact. Peptide fragments of GC determined by MS are shown as black bars above the sequence. The region of divergence between the published GC sequence (Singh et al., 1988) and our sequence is indicated by a black arrow. (B) Comparison of the phosphorylation sites in the KHD of *A. punctulata* GC (ApGC) and mammalian GC-A (Chinkers et al., 1989) and GC-B (Schulz et al., 1989). Phosphorylated residues are highlighted in red, conserved amino acids are in gray, and identical amino acids are in black. rGC, recombinant GC.

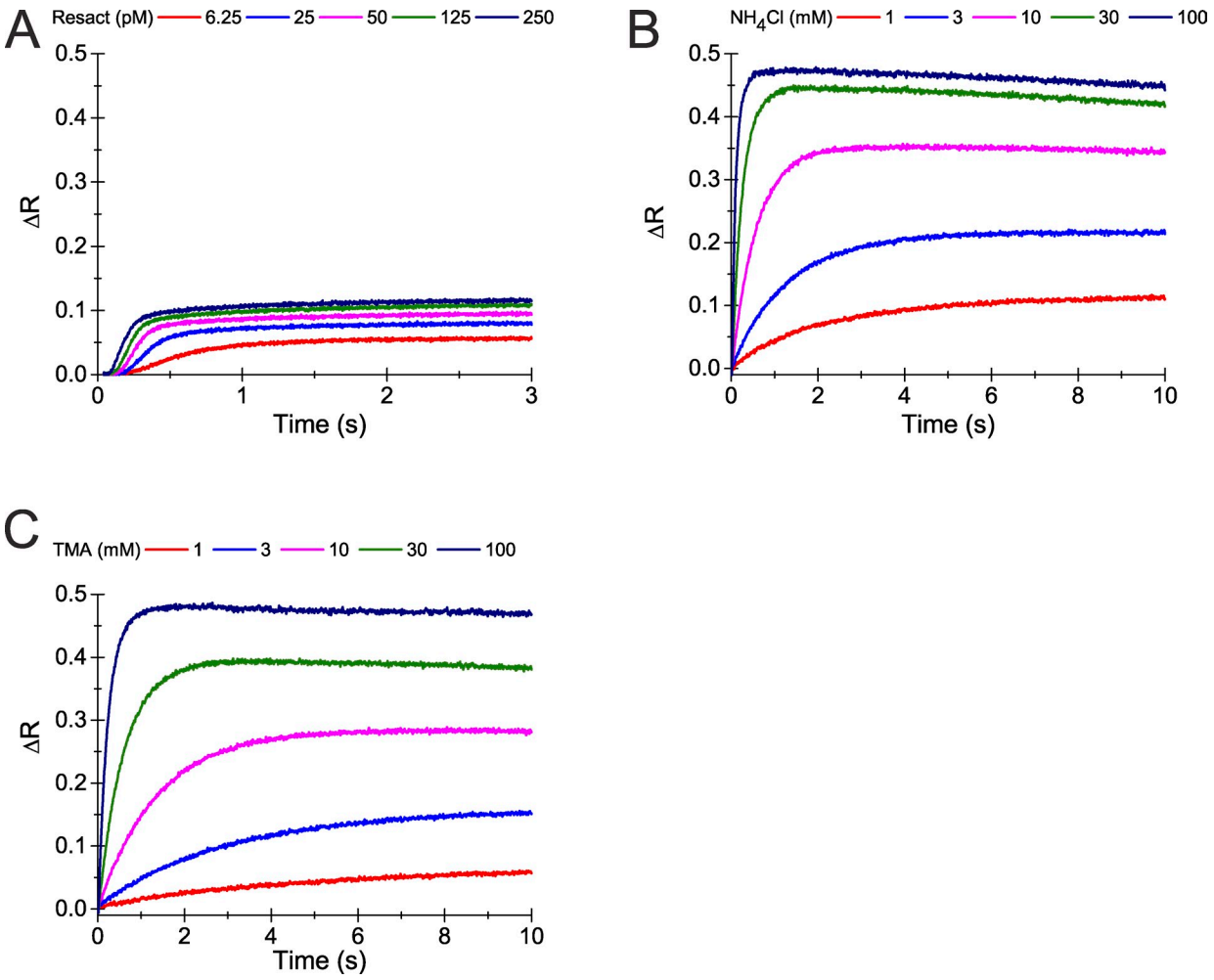

Figure S3. **Changes in pH_i induced by resact, NH_4Cl, or TMA.** (A–C) Sperm were stimulated with different concentrations of either resact (A), NH_4Cl (B), or TMA (C). Changes in pH_i were detected by BCECF. Each trace represents the mean of three recordings. ΔR represents the ratio of fluorescence at 540 and 494 nm; excitation is at 425 nm.

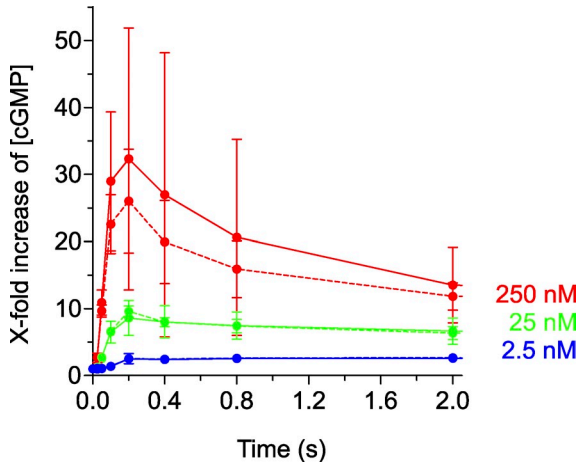

Figure S4. **Resact-evoked cGMP response with and without phosphatase inhibitors.** Time course of cGMP increase was determined by quenched-flow experiments. Sperm were stimulated with resact (2.5, 25, and 250 nM) in the absence (solid lines) and in the presence (broken lines) of 150 nM calyculin (8-min preincubation). Data points represent the means ± SD (nine measurements from three independent experiments).

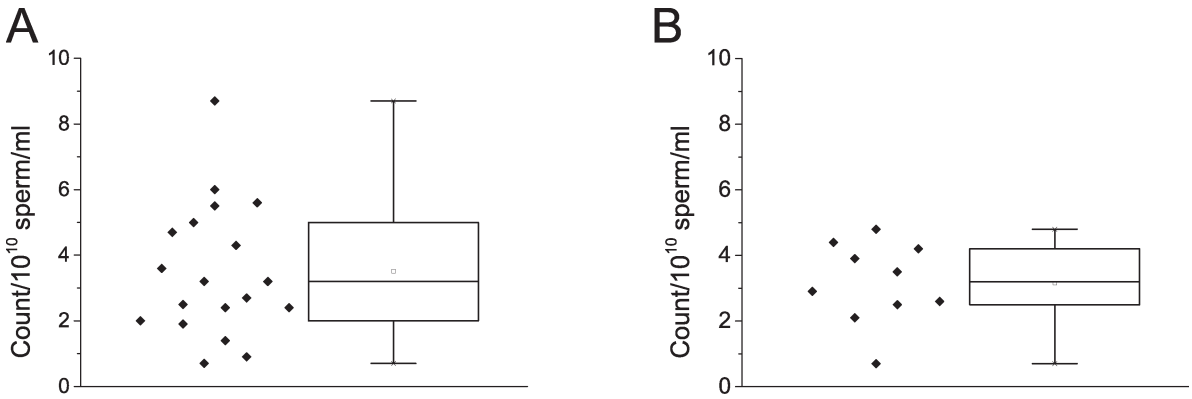

C

	Neubauer chamber	CASY
number of samples	19	10
mean ± SD (sperm ml^{-1})	$3.5 \pm 2.0 \cdot 10^{10}$	$3.2 \pm 1.3 \cdot 10^{10}$
min (sperm ml^{-1})	$0.7 \cdot 10^{10}$	$0.7 \cdot 10^{10}$
median (sperm ml^{-1})	$3.2 \cdot 10^{10}$	$3.2 \cdot 10^{10}$
max (sperm ml^{-1})	$8.7 \cdot 10^{10}$	$4.8 \cdot 10^{10}$

Figure S5. **Statistics of sperm counting.** (A and B) Sperm density was determined either using a Neubauer chamber (A) or a CASY cell counter (B). Each data point represents the sperm density of one animal. Whiskers of the box plot display the values ± 1.5× the interquartile range. Mean values are depicted as open squares. Horizontal lines represent the median, and the dots represent the mean values. (C) Table shows the statistics of sperm density. min, minimum; max, maximum.

Table S1. **Turnover of GC in *A. punctulata* sperm**

Turnover	Conditions	References
cGMP/s		
0.002	Intact sperm stimulated with resact	Suzuki et al., 1984
0.01	Intact sperm stimulated with resact	Shimomura and Garbers, 1986
1.3	Solubilized membrane, basal activity, and $MnCl_2$	Ward et al., 1985
3.1	Solubilized membrane, basal activity, and $MnCl_2$	Ramarao and Garbers, 1985
0.04	Solubilized membrane, stimulated with resact, and $MgCl_2$	Bentley et al., 1986
0.5	Solubilized membrane, basal activity, and $MnCl_2$	Ward et al., 1986
175	Purified GC, basal activity, and $MnCl_2$	Ramarao and Garbers, 1988
0.76	Purified GC, basal activity, and $MgCl_2$	Ramarao and Garbers, 1988

In the literature, turnover values are given in nanomoles of cGMP per minute and milligrams of protein or nanomoles of cGMP per minute and milligram wet weight. To convert these values in cGMP molecules per second, we used the following assumptions: The GC makes up 15% of total membrane proteins. 1 mg of dry sperm contains 10^8 sperm (Ramarao and Garbers, 1985). One sperm cell contains ~300,000 GC molecules. Please note that GC activity probed with $MnCl_2$ in general is 100–200-fold higher than with $MgCl_2$ prevailing in the cell.

Table S2. **Phosphopeptides of the phosphorylated GC**

$[M+H]^+_{exp.}$	$[M+H]^+_{calc.}$	Δ Mass	Missed cleavage	Sequence	Start–end	Phosphorylated sites	Enzyme
		D					
1,424.50	1,424.54	−0.05	0	ESETNSQGFSMK	553–564	S558	Trypsin
1,440.51	1,440.54	−0.03	0	ESETNSQGFSM(ox)K	553–564	S558	Trypsin
1,504.46	1,504.51	−0.05	0	ESETNSQGFSMK	553–564	S558 and S562	Trypsin
1,724.78	1,724.76	0.02	0	SM(ox)VLSAISVISNAEK	565–579	S569 and S575	Trypsin
1,055.46	1,055.48	−0.02	0	SVISNAEKQ	572–580	S572	Elastase
1,319.54	1,319.56	−0.02	0	AISVISNAEKQ	570–580	S572 and S575	Elastase
1,135.42	1,135.44	−0.02	0	SVISNAEKQ	572–580	S572 and S575	Elastase
1,296.60	1,296.62	−0.02	0	SVISNAEKQQI	572–582	S575	Elastase
997.43	997.44	−0.01	0	SNAEKQQI	575–582	S575	Elastase
1,628.72	1,628.80	−0.08	0	SMVLSAISVISNAEK	565–579	S575	Trypsin
1,644.71	1,644.79	−0.09	0	SM(ox)VLSAISVISNAEK	565–579	S575	Trypsin
2,084.01	2,084.09	−0.09	1	VKPPPQKLSQDVLDAAAAR	1,098–1,116	S1106	Trypsin

After in-gel digestion with different proteases, the phosphorylated sequences were identified using a nano-LC–MS/MS. M(ox), oxidation of Met; $[M+H]^+_{exp.}$, experimentally determined mass of the protonated molecular ion; $[M+H]^+_{calc.}$, calculated mass of the protonated molecular ion. Δ Mass refers to the difference of experimentally determined and calculated masses of the protonated molecular ion. The numbers for start–end refer to the amino acid position at the start and end of the peptide, respectively.

Table S3. **Tryptic peptides of dephosphorylated GC**

$[M+H]^+_{exp.}$	$[M+H]^+_{calc.}$	Δ Mass	Missed cleavage	Sequence	Start–end	Phosphorylated sites
		D				
1,344.577	1,344.574	0.002	0	ESETNSQGFSMK	553–564	None
1,360.571	1,360.569	0.002	0	ESETNSQGFSM(ox)K	553–564	None
1,424.544	1,424.541	0.003	0	ESETNSQGFSMK	553–564	S558
1,440.538	1,440.536	0.003	0	ESETNSQGFSM(ox)K	553–564	S558
1,548.831	1,548.831	0.001	0	SMVLSAISVISNAEK	565–579	None
1,564.821	1,564.826	−0.004	0	SM(ox)VLSAISVISNAEK	565–579	None
1,628.798	1,628.797	0.001	0	SMVLSAISVISNAEK	565–579	S575
1,644.794	1,644.792	0.002	0	SM(ox)VLSAISVISNAEK	565–579	S575
1,228.638	1,228.641	−0.003	0	LSQDVLDAAAAR	1,106–1,116	None

After in-gel digestion with different proteases, phosphorylated and the corresponding unphosphorylated peptides were identified using nano-LC–MS/MS. On stimulation by resact, a small fraction of Ser558 and Ser575 remained phosphorylated, whereas all other phosphorylated sites listed in Table S2 were completely dephosphorylated. M(ox), oxidation of Met; $[M+H]^+_{exp.}$, experimentally determined mass of the protonated molecular ion; $[M+H]^+_{calc.}$, calculated mass of the protonated molecular ion. Δ Mass refers to the difference of experimentally determined and calculated masses of the protonated molecular ion. The numbers for start–end refer to the amino acid position at the start and end of the peptide, respectively.

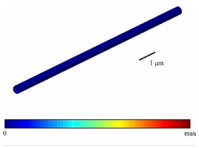

Video 1. **Simulation of cGMP diffusion along the sperm flagellum.** Diffusion of cGMP from a point source along the flagellum was calculated by using Eqs. 5–8 (Materials and methods). The concentration of cGMP is depicted in false colors. max conc, maximum concentration.

References

Bentley, J.K., H. Shimomura, and D.L. Garbers. 1986. Retention of a functional resact receptor in isolated sperm plasma membranes. *Cell*. 45:281–288. http://dx.doi.org/10.1016/0092-8674(86)90392-2

Chinkers, M., D.L. Garbers, M.S. Chang, D.G. Lowe, H.M. Chin, D.V. Goeddel, and S. Schulz. 1989. A membrane form of guanylate cyclase is an atrial natriuretic peptide receptor. *Nature*. 338:78–83. http://dx.doi.org/10.1038/338078a0

Ramarao, C.S., and D.L. Garbers. 1985. Receptor-mediated regulation of guanylate cyclase activity in spermatozoa. *J. Biol. Chem.* 260:8390–8396.

Ramarao, C.S., and D.L. Garbers. 1988. Purification and properties of the phosphorylated form of guanylate cyclase. *J. Biol. Chem.* 263:1524–1529.

Schulz, S., M. Chinkers, and D.L. Garbers. 1989. The guanylate cyclase/receptor family of proteins. *FASEB J.* 3:2026–2035.

Shimomura, H., and D.L. Garbers. 1986. Differential effects of resact analogues on sperm respiration rates and cyclic nucleotide concentrations. *Biochemistry*. 25:3405–3410. http://dx.doi.org/10.1021/bi00359a046

Singh, S., D.G. Lowe, D.S. Thorpe, H. Rodriguez, W.-J. Kuang, L.J. Dangott, M. Chinkers, D.V. Goeddel, and D.L. Garbers. 1988. Membrane guanylate cyclase is a cell-surface receptor with homology to protein kinases. *Nature*. 334:708–712. http://dx.doi.org/10.1038/334708a0

Suzuki, N., H. Shimomura, E.W. Radany, C.S. Ramarao, G.E. Ward, J.K. Bentley, and D.L. Garbers. 1984. A peptide associated with eggs causes a mobility shift in a major plasma membrane protein of spermatozoa. *J. Biol. Chem.* 259:14874–14879.

Ward, G.E., C.J. Brokaw, D.L. Garbers, and V.D. Vacquier. 1985. Chemotaxis of *Arbacia punctulata* spermatozoa to resact, a peptide from the egg jelly layer. *J. Cell Biol.* 101:2324–2329. http://dx.doi.org/10.1083/jcb.101.6.2324

Ward, G.E., G.W. Moy, and V.D. Vacquier. 1986. Dephosphorylation of sea urchin sperm guanylate cyclase during fertilization. *Adv. Exp. Med. Biol.* 207:359–382.